Chin. Geogra. Sci. 2022 Vol. 32 No. 1 pp. 79−92
https://doi.org/10.1007/s11769-021-1251-3

Springer Science Press
www.springerlink.com/content/1002-0063

Impacts of Urban Expansion on the Urban Thermal Environment: A Case Study of Changchun, China

YANG Limin[1, 2], LI Xiaoyan[1], SHANG Beibei[1]

(1. *College of Earth Sciences*, *Jilin University*, *Changchun* 130012, *China*; 2. *College of Public Administration*, *Nanjing Agricultural University*, *Nanjing* 210095, *China*)

Abstract: Urbanization, especially urban land expansion, has a profound influence on the urban thermal environment. Cities in Northeast China face remarkably uneven development and environmental issues, and thus it is necessary to strengthen the diagnosis of thermal environmental pressure brought by urbanization. In this study, multi remote sensing imageries and statistical approaches, involving piecewise linear regression (PLR), were used to explore urban expansion and its effects on the thermal environment of Changchun City in Jilin Province, China. Results show that Changchun experienced rapid urban expansion from 2000 to 2020, with urban built-up areas increasing from 171.77 to 525.14 km^2. The area of the city's urban heat island (UHI) increased dramatically, during both day and night. Using PLR, a positive linear correlation of built-up density with land surface temperature (LST) was detected, with critical breakpoints of 70%−80% during the daytime and 40%−50% at nighttime. Above the thresholds, the magnitude of LST in response to built-up density significantly increased with intensifying urbanization, especially for nighttime LST. An analysis of the relative frequency distributions (RFDs) of LST reveals that rapid urbanization resulted in a significant increase of mean LST in newly urbanized areas, but had weak effects on daytime LST change in existing urban area. Urban expansion also contributed to a constant decrease of spatial heterogeneity of LST in existing urban area, especially at daytime. However, in newly urbanized areas, the spatial heterogeneity of LST was decreased during the daytime but increased at nighttime due to urbanization.

Keywords: urban expansion; urban thermal environment; urban heat island (UHI); remote sensing; Changchun; China

Citation: YANG Limin, LI Xiaoyan, SHANG Beibei, 2022. Impacts of Urban Expansion on the Urban Thermal Environment: A Case Study of Changchun, China. *Chinese Geographical Science*, 32(1): 79−92. https://doi.org/10.1007/s11769-021-1251-3

1 Introduction

Over the last few decades, urban expansion has been the dominant form of urban development at local, regional, and global scales (Li et al., 2018). This has significantly changed characteristics of urban environment and transformed natural ecosystems into semi-natural or even non-natural ecosystems (Peng et al., 2016; Hu et al., 2017). As a result, cities are places of increasingly ecological environmental problems—like heat risk due to the urban heat island (UHI) effect—which is among the most important factors currently affecting the health of urban residents (Fernández and Wu, 2016; Chapman et al., 2017; Wang et al., 2018).

The UHI, a phenomenon defined as urban areas being warmer than the surrounding rural areas, is seen in cities worldwide (Li et al., 2017; Pal and Ziaul, 2017). UHI can be placed into four categories: surface urban heat islands (SUHI), boundary-layer heat islands (BLHI), canopy-layer heat islands (CLHI), and subsurface

Received date: 2021-04-15; accepted date: 2021-08-02
Foundation item: Under the auspices of the Natural Science Foundation of Jilin Province (No. 20200201048JC)
Corresponding author: LI Xiaoyan. E-mail: lxyan@jlu.edu.cn

urban heat islands (SSUHI) (Zhang et al., 2009; Menberg et al., 2013). Recent UHI studies have concentrated on land surface temperature (LST) or the SUHI effect, since it is the most direct manifestation of urban thermal environment, and freely accessible and available high-resolution remote sensing images provide a valuable and reliable data source for LST studies (Peng et al., 2016; Deilami et al., 2018; Li et al., 2018).

Previous studies have extensively investigated the UHI/LST dynamics and explored effects of multiple factors on the generation of the UHI and its variance (Deilami et al., 2018). The rapid urbanization process, the increase needs of manufactured materials and heating/cooling energy, coupled with anthropologic heat emissions, have large impacts on urban temperatures, exacerbating UHI effect as well as making urban areas warmer (Mohajerani et al., 2017; Sun et al., 2018). Among these factors, urbanization, which is principally associated with size, density, diversity, and spatial structure pattern, is the most significant cause of UHI effect, in which both densification and sprawl processes may exhibit and intensify UHI effects (Tsai, 2005; Debbage and Shepherd, 2015; Mohajerani et al., 2017). Urban scale has a positive association with UHI intensity, and larger cities exacerbate UHI threats (Tan and Li, 2015). UHI effect is more strongly associated with landscape composition and configuration, of which the constant increase in impervious surfaces (including built-up areas, asphalt pavements and roads) and the reduction in natural vegetation are widely reported as the key variables to explain UHI variance (Dobrovolný, 2013; Debbage and Shepherd, 2015; Morabito et al., 2016; Estoque et al., 2017; Deilami et al., 2018). Urban areas are always characterized by the greatest degree of soil sealing and the maximum built-up density, where vegetation cover areas are small, typically close to the minimum, and thereby, urban areas are more sensitive to heat-related issues (Mathew et al., 2017; Singh et al., 2017). Therefore, the quantitative analysis of urban expansion and the investigation of its effects on LST variation and UHI effect are valuable for urban thermal environmental research.

Assessments of effects of urban expansion on the thermal environment have been carried out in some Asian cities over the last two decades, revealing that UHI effect exists in different climate regions at different scales. Li et al. (2019) found that higher daytime SUHI values occurred in hot-humid South China and the cold-humid northeastern China. Since spatial heterogeneity is the fundamental characteristic of LST that is intrinsically related to location, it is worth analyzing individual cities in Northeast China—the so-called Chinese snow climate cities (Zhou et al., 2015; Mohajerani et al., 2017; Yang et al., 2020). Besides, UHI effects exist at any time of day and night, but mechanisms affecting UHI are complex and vary between day and night time (Azevedo et al., 2016). Current studies mainly concentrated in eastern coastal areas, but the varying responses of the UHI at daytime and nighttime to urbanization for cities in Northeast China is limited. In addition, although the sustainability of urban development has been promoted in the 21st century, cities especially in Northeast China still face remarkably uneven development and environmental issues (Kuang, 2020). Therefore, it is more necessary to strengthen the diagnosis of thermal environmental pressure brought by urbanization in these northeastern cities. Many researches have revealed a positive relationship between LST and some major indicators of urbanization—like built-up areas or the normalized difference built-up index (NDBI), but the identification of the impact thresholds in this relationship is inadequate. Given this, taking Changchun City, China as a case study, the spatiotemporal effects of urban expansion on the urban thermal environment were analyzed via multiperiod satellite images and statistical approaches, and the responses of LST during both day and night to built-up density were quantitatively measured based on piecewise linear regression (PLR) analysis, to help to seek a reasonable scale for developing effective mitigation measures and strategies. The main objectives of the study were as follows: 1) to depict the process of urban land expansion in Changchun from 2000 to 2020; 2) to analyze the characteristics of the thermal environment in 2000, 2010 and 2020, and 3) to explore the impacts of urban expansion on urban thermal environment.

2 Materials and Method

2.1 Study area

Changchun, the capital city of Jilin Province, China (124°18′E–127°02′E, 43°05′N–45°15′N) lies in the central part of the Songneng Plain, with an elevation ranging from 67 m to 386 m within its administrative region. It has a mid-latitude location and an East Asian

monsoon climate; its winters are extremely long, cold, windy, and dry, while the summers are hot, humid, and short. The average annual precipitation is 561.6 mm, concentrated between June and August; the annual average temperature is 4.6°C, with a monthly average temperature of –15.1°C in January and 23.1°C in July. The study area was Changchun City proper, which contains Chaoyang, Nanguan, Kuancheng, Erdao, and Luyuan districts, with a total area of 3.5×10^2 km^2 (Fig. 1). Over the last 20 yr, Changchun has experienced rapid urbanization and population aggregation, inevitably affecting its urban thermal environment.

2.2 Data sources

In this study, in order to reduce potential bias due to using LST data from a single time, 54 daytime and nighttime 8-day composite LST time series products (MOD11A2) were obtained for July and August in 2000, 2010 and 2020, downloaded from Earthdata website (https://search.earthdata.nasa.gov/search). MODIS/Terra LST products provide two snapshots for each day at about 10:50 (day) and 22:10 (night) with a spatial resolution of 1 km.

Landsat 5 Thematic Mapper (TM) images (30 m) at Aug. 12, 2001 and Sept. 22, 2010, and Landsat 8 Operational Land Imager (OLI) images (30 m) at Sept. 15, 2019, were used in this study. All images, taken under clear atmospheric conditions and low cloud coverage of less than 10%, were downloaded from the NASA website (https://www.nasa.gov/), and were preprocessed by atmospheric corrections, radiometric corrections, layer-stacking, and subsetting using ENVI 5.3 software (Exelis Inc., Boulder, CO, USA) to extract land cover information.

2.3 Methods

2.3.1 Extraction and spatial analysis of urbanization

The spectral index method was used to classify land cover information. The index-based built-up index (IBI), proposed by Xu (2008), was imported for rapid built-up extraction with manual calibration. The index is constructed from three thematic indices: the soil-adjusted vegetation index (SAVI), the modified normalized difference water index (MNDWI), and the normalized difference built-up index (NDBI), representing three urban generalization components of vegetation, water, and built-up land, respectively (Sekertekin et al., 2018). The equations used to calculate these indices were as follows:

$$IBI = \frac{NDBI - (SAVI + MNDWI)/2}{NDBI + (SAVI + MNDWI)/2} \quad (1)$$

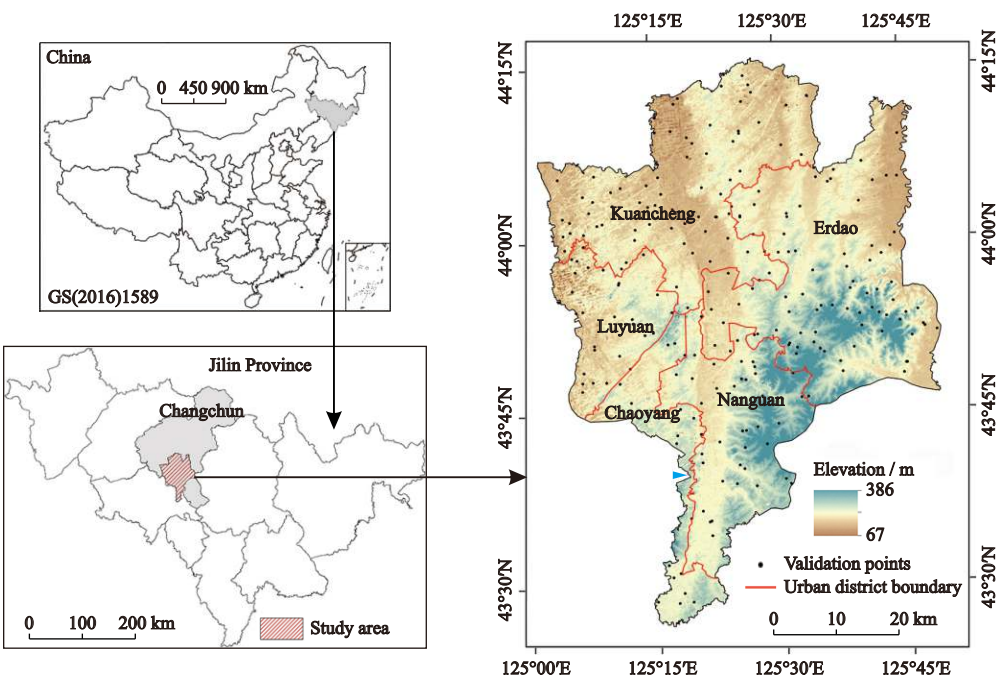

Fig. 1 Geographical location of Changchun, China and validation points of land cover classification

$$SAVI = \frac{(NIR - RED)(1 + L)}{(NIR + RED + L)} \quad (2)$$

$$MNDWI = \frac{GREEN - SWIR}{GREEN + SWIR} \quad (3)$$

$$NDBI = \frac{SWIR - NIR}{SWIR + NIR} \quad (4)$$

where *GREEN*, *RED*, *NIR* and *SWIR* refer to the surface reflectance values of bands 2, 3, 4, and 5 for Landsat-5 TM images, and those of bands 3, 4, 5, and 6 for Landsat-8 OLI images. The correction factor *L*, used in the calculation of SAVI, can take values from 0 to 1, in order to reduce soil noise problems for a wide range of vegetation densities (Huete, 1988).

Historical high-resolution images from Google Earth™ were used as reference layers to assess classification accuracy. The 251 random points were generated to validate agreement of classification results between remote sensing imagery and the reference data (Fig. 1). The interpretation accuracy was 83.27% in 2000, 85.26% in 2010, and 90.84% in 2020, indicating that the classification process was reliable.

Further, referring to Zhou et al. (2016), we defined the scope of urban and suburban areas by segmentation thresholds of 50% and 25% based on built-up density for each MODIS LST pixel, which was produced using a 33 × 33 moving windows based on 30 m built-up land maps and was resampled to 1 km for consistency of the LST data (Fig. 2). The urban area was usually covered by built-up land, with many gaps caused by green spaces, water, and even the agriculture lands, while suburban area was mainly covered by cultivated vegetation besides built-up land (Zhou et al., 2016; Yue et al., 2019).

The urbanization intensity index (UII) is recognized as a critical indicator in reflecting the dynamics of urban expansion (Yeh and Huang, 2009; Li et al., 2017). In this study, the UII values were calculated based on MODIS LST data with 1-km resolution via the following equation (Eq. (5)):

$$UII_i = \frac{UA_{i,t+n} - UA_{i,t}}{n \times TA_i} \times 100 \quad (5)$$

where UII_i refers to the urbanization intensity for pixel *i* from time *t* to *t* + *n*, *n* is the time quantum, $UA_{i,t}$ and $UA_{i,t+n}$ represent areas of built-up land at time *t* and *t* + *n*, respectively, and TA_i is the area of the pixel *i*.

2.3.2 *NLST calculation and UHI measurement*

After eliminating invalid pixels with the quality control (QC) data, the mean LST during both daytime and nighttime were calculated to reduce potential problems with monthly variation. Further, in order to make it easier to compare LST differences between years, the normalized land surface temperature (NLST) was calculated via the following equation (Yang et al., 2017) (Eq. (6)):

$$NLST = \frac{LST_i - LST_{\min}}{LST_{\max} - LST_{\min}} \quad (6)$$

where *NLST* is the normalized LST value of pixel *i*, LST_i is the primary LST of pixel *i*, $LST_{\max}$ and $LST_{\min}$ refer to the maximum and minimum LSTs of the study area, respectively.

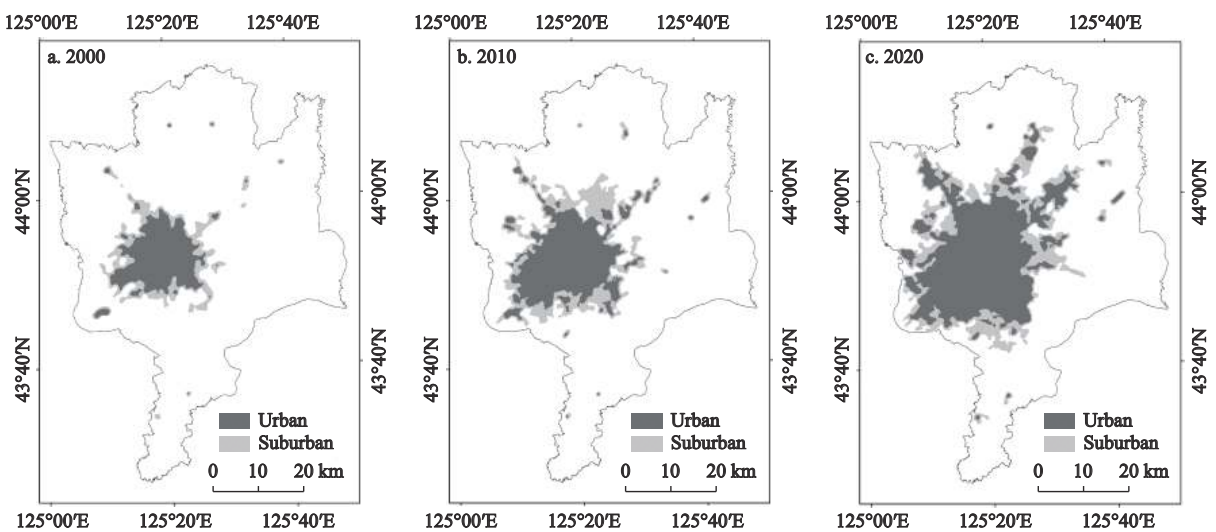

Fig. 2 Urban and suburban areas in the proper of Changchun City, China

The UHI intensity was calculated to qualify the magnitude of the temperature differences (namelyΔT), by subtracting the average NLST over the suburban areas from that of urban areas (Schwarz et al., 2011). As described by Meng et al. (2018), UHI can be divided into grades I, II, III and IV, with grade IV representing the most intensive UHI effect (Table 1). The UHI intensity equation was as follow (Eq. (7)):

$$\Delta T = NLST_{\text{urban}} - NLST_{\text{suburban}} \tag{7}$$

where ΔT refers to the UHI intensity, $NLST_{\text{urban}}$ refers to the average *NLST* amongst urban area, and $NLST_{\text{suburban}}$ is the average NLST over the surrounding suburban area.

2.3.3 Piecewise linear regression (PLR)

The effectiveness of linear correlation in identifying relationships between landscape indicators and LST has been widely acknowledged (Deilami et al., 2018). However, since the actual influence may be complex and not always linear, piecewise linear regression (PLR), being considered more accurate, is suitable for partitioning the variables involved in a nonlinear relationship into intervals over which the relationship can be considered linear (Liu et al., 2018).

In this study, PLR was used to analyze the correlation of built-up density and NLST during the daytime and nighttime. The boundaries of the intervals are called 'breakpoints', or thresholds (Peng et al., 2017). After testing the scale effects on results of spatial analysis, the 2 km × 2 km unit of analysis was selected since it retains details without too much noise. Further, we divided built-up density into intervals of 5%, and set the range as 5%–100% to reduce bias caused by redundant samples. The two-segment regression equation, for instance, was described as follows (Eq. (8)):

$$y = \begin{cases} \beta_0 + \beta_1 x + \varepsilon_x & x \le a \\ \beta_0 + \beta_1 x + \beta_2 (x - a) + \varepsilon_x & x > a \end{cases} \tag{8}$$

Table 1 Urban Heat Island (UHI) classification criteria

Grade	Calculation method
I	$NLST_{\text{suburban}} \le NLST < (NLST_{\text{suburban}} + 0.5\Delta T)$
II	$(NLST_{\text{suburban}} + 0.5\Delta T) \le NLST < (NLST_{\text{suburban}} + \Delta T)$
III	$(NLST_{\text{suburban}} + \Delta T) \le NLST < (NLST_{\text{suburban}} + 1.5\Delta T)$
IV	$NLST \ge (NLST_{\text{suburban}} + 1.5\Delta T)$

Note: NLST is the normalized daytime/nighttime LST (land surface temperature) of each pixel, for each year

where y refers to the NLST, β_0 is a constant, β_1 and β_2 are the slope below and above the breakpoint, respectively, x is built-up density, a is the breakpoint (or threshold), and ε_x is the residual.

3 Results

3.1 Spatiotemporal patterns of urban expansion

Changchun had experienced rapid urban expansion over the last 20 yr (Fig. 3 and Table 2). The urban built-up area increased from 171.77 km^2 in 2000 to 288.48 km^2 in 2010, and to 525.14 km^2 in 2020, at an annual expansion rate of 6.23% and 8.20%, respectively (Fig. 3a). During this urban expansion period, the heterogeneity in urbanization intensity within urban area was reflected (Fig. 3b and Fig. 3c). The newly urbanized built-up area with UII greater than 2 accounted for 37.97% in 2000–2010 periods, and 40.26% in 2010–2020 period, respectively, which spread the peri-urban areas especially in the southwest and northeast.

3.2 Dynamics of the thermal environment

The daytime UHI intensity was 0.27, 0.22 and 0.15 in 2000, 2010 and 2020, respectively, a significant decline was observed; the UHI intensity at night was 0.25, 0.28 and 0.24, for the same years respectively (Table 3). Spatially, areas of grades I to IV heat island for both daytime and nighttime significantly increased since 2000 (Table 4 and Fig. 4). In particular, the area ratio for the grade IV heat islands during the daytime increased from 0.99% in 2000 to 2.53% in 2010, and to 6.13% in 2020, a growth of 1.54% and 3.6%, respectively. For nighttime, the percentage of the grade IV heat islands area increased from 1.98% in 2000 to 4.80% in 2010, and to 8.13% in 2020, with a increase of 2.82%, and 3.33%, respectively.

3.3 Response of NLST to built-up density

Overall, statistically significant linear relationship ($P <$ 0.001) between built-up density and NLST during both daytime and nighttime was observed in each study year. Using PLR, thresholds were identified in impacts of urban land expansion on the NLST (Fig. 5). For daytime NLST in 2000, the threshold value was 75%–80%, and the linear correlation values were 0.036 below and 0.023 above the threshold, respectively. A positive lin-

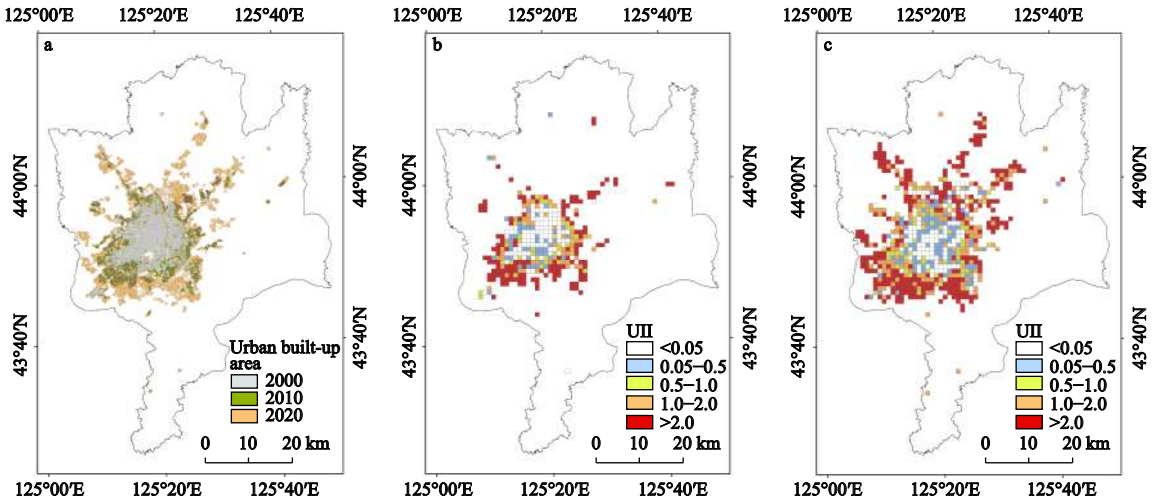

Fig. 3 Urban built-up area in 2000, 2010 and 2020 (a), and the urbanization intensity index (UII) for 2000–2010 (b) and 2010–2020 (c) in proper of Changchun City, China. UII is urbanization intensity

Table 2 Statistics for urban expansion from 2000 to 2020 in Changchun City, China

Year	Area / km^2	Annual expansion rate / %	Proportion of UII / %				
			<0.05	0.05–0.50	0.50–1.00	1.00–2.00	>2.00
2000	171.77	6.23	25.40	12.30	9.63	14.71	37.97
2010	288.48	8.20	16.19	14.47	7.89	21.20	40.26
2020	525.14						

Note: UII is urbanization intensity

Table 3 Statistics for urban heat island (UHI) intensity in 2000, 2010 and 2020 in Changchun City, China

Day/Night	2000			2010			2020		
	$NLST_{urban}$	$NLST_{suburban}$	ΔT	$NLST_{urban}$	$NLST_{suburban}$	ΔT	$NLST_{urban}$	$NLST_{suburban}$	ΔT
Daytime	0.79	0.52	0.27	0.70	0.48	0.22	0.69	0.54	0.15
Nighttime	0.66	0.41	0.25	0.66	0.38	0.28	0.58	0.34	0.24

Notes: ΔT refers to the UHI intensity, $NLST_{urban}$ and $NLST_{suburban}$ refer to the average $NLST$ amongst urban area and the surrounding suburban area, respectively

Table 4 Percentage of total area of urban heat island (UHI) in 2000, 2010 and 2020 in Changchun City, China / %

Grade	2000		2010		2020	
	Daytime	Nighttime	Daytime	Nighttime	Daytime	Nighttime
I	4.18	4.69	6.40	10.60	9.29	19.08
II	2.20	3.44	3.71	4.80	7.79	7.46
III	3.22	2.55	3.94	3.68	5.62	4.96
IV	0.99	1.98	2.53	4.80	6.13	8.13

Note: Grades I to IV see Table 1

ear correlation was found between built-up density and daytime NLST in 2010, without exhibiting any thresholds; on average, a 5% increase of built-up density approximately increased daytime NLST by 0.031. The daytime NLST response to built-up density had two thresholds in 2020 (45%–50% and 70%–75%), with the slopes of 0.034 below the 45%–50% threshold and 0.038 above the 70%–75% threshold, respectively. Whereas, in such two thresholds range, the increasing built-up density had a weak positive effect on daytime

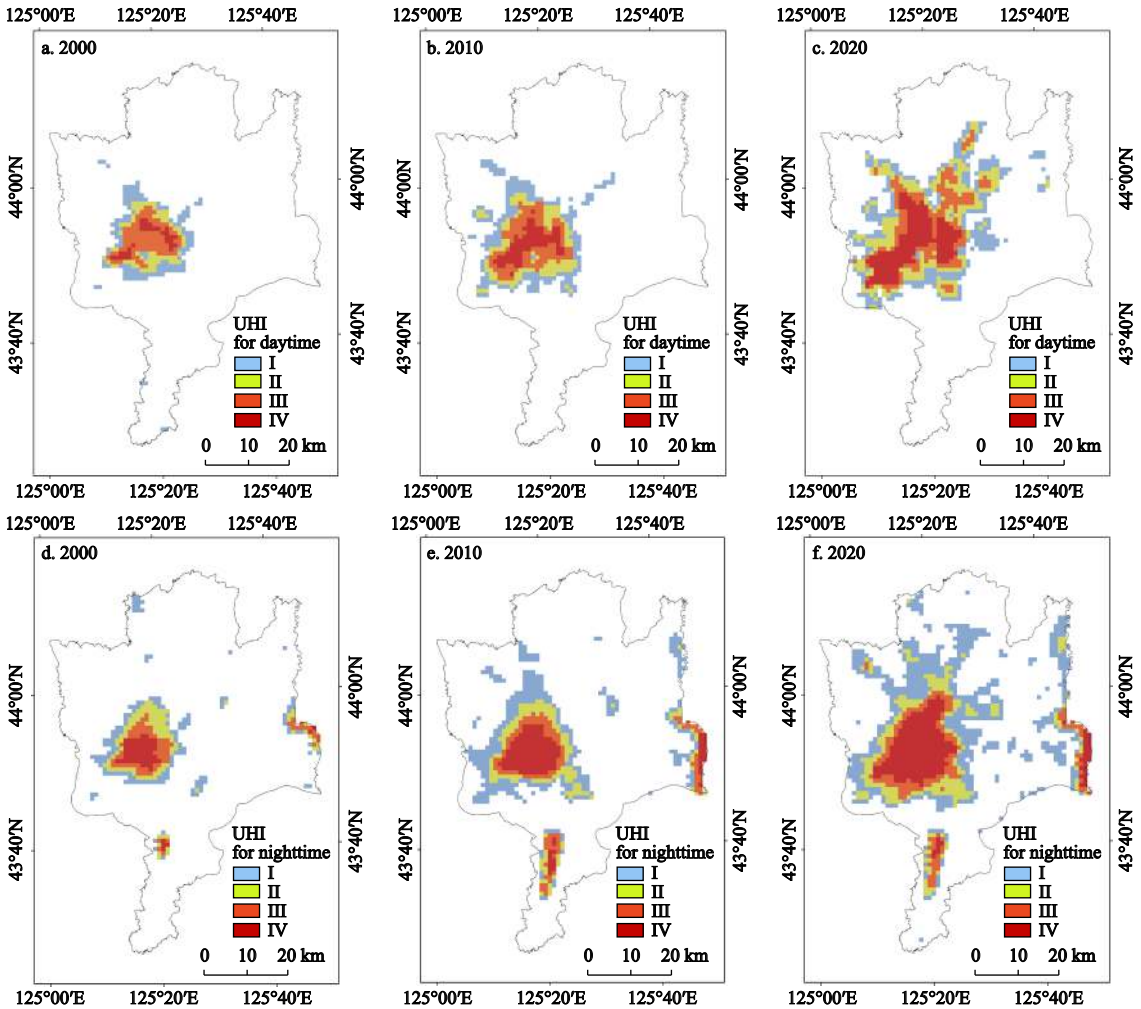

Fig. 4 The urban heat island (UHI) maps for daytime (a, b, c) and nighttime (d, e, f) in 2000, 2010 and 2020 in proper of Changchun City, China. Grades I to IV see Table 1

NLST, with the linear correlation value of 0.014.

For nighttime NLST, the threshold values were 45%–50% in 2000, 45%–50% in 2010, and 40%–45% in 2020, respectively. Below each threshold, the linear correlation values were 0.027, 0.019, and 0.009 in 2000, 2010 and 2020, respectively. However, above the thresholds, the slope of the linear ralationship were 0.036, 0.048 and 0.048, respectively. During the period from 2000 to 2020, the response of NLST to built-up density during both daytime and nighttime each had a threshold (40%–50% at night and 70%–80% at day, respectively), above which NLST increased rapidly with intensifying urbanization, especially at nighttime.

3.4 Impacts of urban expansion on NLST

The relative frequency distributions (RFDs), the mean and standard deviations of the NLST were used to further analyze the varying effects of urban expansion on the NLST during the daytime and nighttime (Fig. 6 and Table 5). The urban area in 2000 was defined as zone 1, and newly urbanized area in 2010, 2020 were defined as zone 2 and zone 3, respectively. During 2000–2020 period, the standard deviation of NLST within zone 1 significantly decreased by 0.063 at daytime and 0.053 at nighttime, suggesting that the spatial heterogeneity of NLST in existing urban area decreased with intensifying urbanization. In addition, the mean daytime NLST within zone 1 were 0.785, 0.758 and 0.775 in 2000, 2010 and 2020, respectively; however, the mean nighttime NLST significantly increased from 0.657 to 0.795, with an obvious increase in the relative frequency of NLST above 0.7. Within zone 2, the relative frequency of NLST above 0.5 during both daytime and nighttime

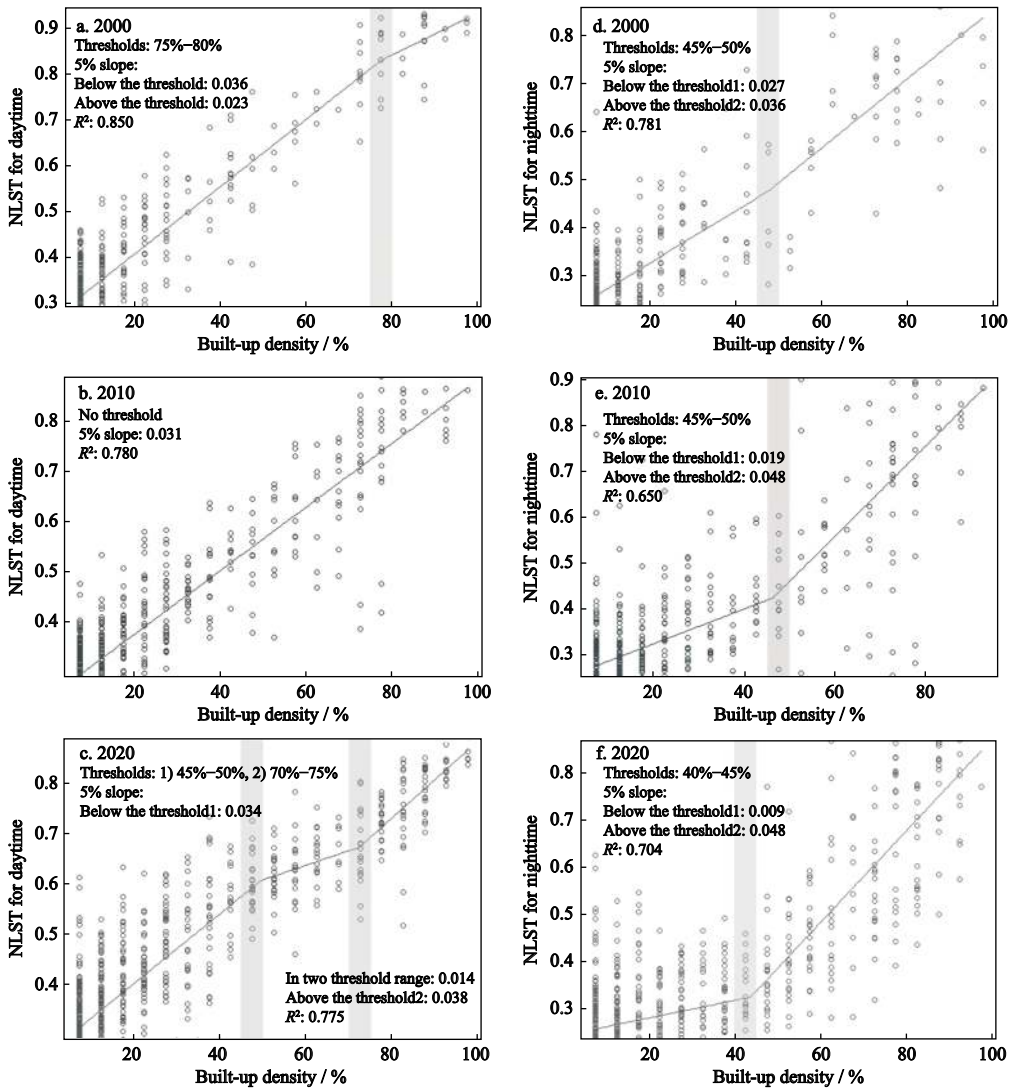

Fig. 5 Thresholds and the correlation of built-up density with the NLST in daytime (a, b, c) and nighttime (d, e, f) using piecewise linear regression (PLR) from 2000 to 2020 in proper of Changchun City, China ($P < 0.001$). The grey stripes represent the thresholds

significantly increased during 2000–2020. Within zone 3, the RFDs of daytime and nighttime NLST had a single peak, and the NLST values at their highest relative frequency significantly increased from 2000 to 2020, especially at daytime. Besides, within zone 2 and zone 3, the mean NLST increased by 0.196 and 0.246 during the daytime, and 0.163 and 0.146 at nighttime, respectively. This suggested that rapid urban expansion resulted in a significant increase of NLST in newly urbanized areas, especially for daytime NLST. In addition, the standard deviation of NLST in newly urbanized areas decreased during the daytime, while increased at nighttime during 2000–2020. That is, an opposite effect of urban expansion on the spatial heterogeneity of NLST has occurred between day and night in newly urbanized areas.

4 Discussion

4.1 Dynamic characteristics of urban land expansion

Changchun has undergone rapid urban land expansion under globalization and rapid socioeconomic development since 2000 (Kuang, 2020). The annual expansion rate of urban built-up land from 2000 to 2010 (6.23%) was higher than the mean value for Northeast China (3.61% during 2000–2005, and 7.59% during 2005–2010) over the same period (Kuang et al., 2016). During 2010–2020, the annual expansion rate increased to 8.20%, indicating an accelerating development

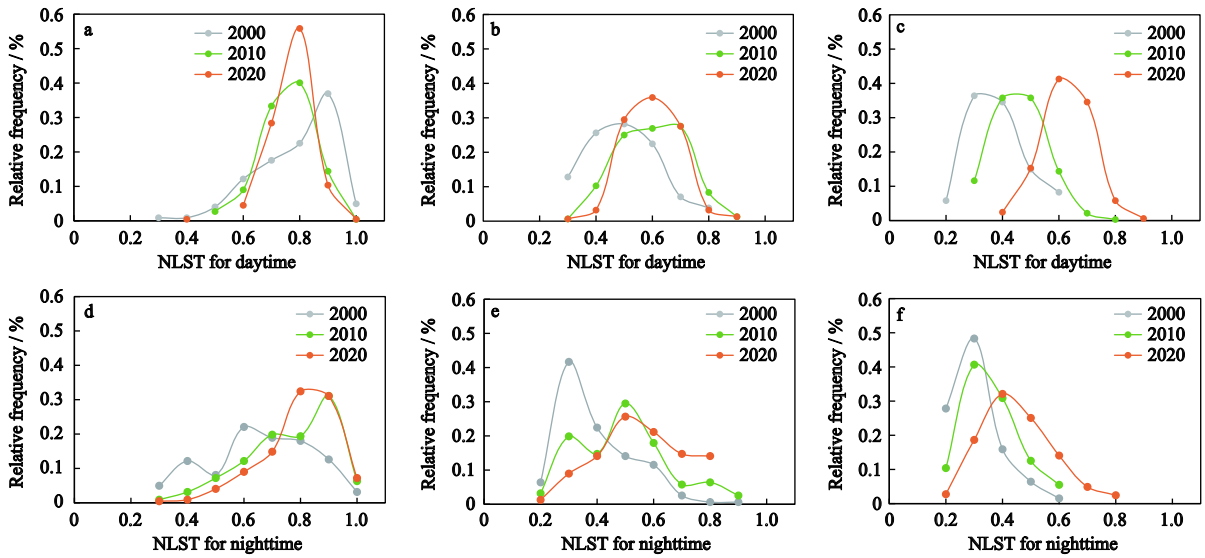

Fig. 6 The relative frequency distributions of the normalized land surface temperature (NLST) in daytime (a, b, c) and nighttime (d, e, f) in zone 1, zone 2, zone 3 from 2000 to 2020 in proper of Changchun City, China. The urban area in 2000 was defined as zone 1, and newly urbanized area in 2010, 2020 were defined as zone 2 and zone 3, respectively

Table 5 Statistics for the normalized land surface temperature (NLST) within zone 1, zone 2 and zone 3 from 2000 to 2020

Zone	Day/Night	2000		2010		2020	
		Mean	Standard deviation	Mean	Standard deviation	Mean	Standard deviation
Zone 1	Daytime	0.785	0.138	0.758	0.091	0.775	0.075
	Nighttime	0.657	0.179	0.766	0.154	0.795	0.126
Zone 2	Daytime	0.501	0.128	0.602	0.120	0.697	0.097
	Nighttime	0.395	0.130	0.498	0.161	0.558	0.154
Zone 3	Daytime	0.384	0.099	0.459	0.091	0.630	0.084
	Nighttime	0.304	0.085	0.363	0.098	0.450	0.124

Note: Meanings of zone 1, 2, 3 see Fig.6

(Fig. 3 and Table 3). The city's development process is strongly controlled by socio-economic factors and planning policies, which have pronounced effects on urban expansion trajectories, directions, and characteristics (Kuang and Yan, 2018). The Northeast China, once the most highly developed region as the traditional industrial and grain base of China, went through a remarkable economic recession in the 1990s due to tremendous challenges of resource depletion, environmental pollution, and business reconstruction, resulting in urbanization falling behind that of the southern coastal cities. In response to the 'Revitalization of the Old Industrial Bases in Northeast China' policy proposed in 2003, the Changchun Hi-Tech Zone and the Changchun Automotive Economic Trade and Development Zone entered the 'second venture' stage that developed a large area to the southeast. Chen et al. (2018) found that urban land in Changchun increased faster during 2000–2010 than during the 1990s. From 2010 to 2020, the spatial pattern of urban land was significantly reshaped by a shift in focus from the southwest to the northeast. The new town on the city's north side was developed quickly as part of a plan to break the dual economy of the region.

4.2 Urban thermal environment characteristics

The UHI effect (through spatiotemporal changes in LST) is an important climatic aspect of thermal environment assessment. Research of UHI requires a consistent and reliable dataset to derive the LST and subsequently UHI intensity. MODIS LST data has its effectiveness of monitoring urban temperature, and such composite LST data can reduce time required to derive LST as well as

improve the reliability of LST (Chapman et al., 2017; Duncan et al., 2019). However, the advantage of MODIS images may be compromised by its low spatial resolution, which may not suitable for detailed LST/UHI applications (Chapman et al., 2017).

In this study, we found that urban areas always exhibited the most intensive UHI effect, with many new hot spots appearing, enlarging, and gathering that creating a larger heat island during both daytime and nighttime from 2000 to 2020 (Fig. 4 and Table 4). However, a larger UHI region does not mean a stronger UHI intensity. The UHI effect and its intensity in cities are significantly affected by the region geographic features, climatic conditions, seasonal and diurnal variations (Mohajerani et al., 2017). The UHI intensity and the LST spatial pattern of Changchun, a typical snow-climate city, has huge monthly and seasonal changes (Yang et al., 2020). The LST data in July and August more closely corresponds to the time of maximum temperatures of Changchun city, and the UHI intensity is much higher for these summer days. Besides, the UHI effect exists at any time in day and night, but its intensity is much intense at night due to the thermal capacity of materials (e.g., concrete, asphalt) and its specific cooling process, i.e., cities absorb a high amount of heat during the day and release it slowly over night (Azevedo et al., 2016; Chapman et al., 2017). In our case, we found a significant decrease in daytime UHI intensity from 0.27 to 0.15 during 2000–2020 (Table 3), and such phenomenon may be highly associated with the underlying land cover changes. Yang et al. (2017) found that the area of UHI regions increased, but the hot spots and the distribution of the higher and highest LST zones were less concentrated than before, and explained that new land of relatively slow development was incorporated into urban regions that help to disperse the LST. In addtion, the UHI intensity varies based on different definitions and measurements. Yang et al. (2017) found that the UHI intensity—by subtracting the mean NLST for rural areas from that for urban areas—decreased from 2000 to 2014; however, a reverse trend of UHI was found in the same period by defining the inner UHI intensity, which obtained by subtracting the mean NLST for rural areas from that for inner urban areas. Besides, Huang et al. (2014) classified heat island intensity according to human body temperature thermal comfort and physiological responses, and believed it to be a usable research method.

4.3 Effects of urban expansion on urban thermal environment

Many studies have found that urban expansion has a significant impact on the urban thermal environment, and in particular the change of built-up environment has been shown to be one of the major causes of LST fluctuations globally (Sun et al., 2015; Li et al., 2018). In this study, we found that the spatial distribution of heat island during the daytime, especially the grades II to IV heat island over the study area, appeared to be highly linked to urban expansion from 2010 to 2020 (Fig. 4). In contrast, the spatial pattern of UHI at nighttime in the studied period have a nearly concentric shape, which is significantly differed from that for daytime. This suggested that the spatial distribution of heat island at nighttime in Changchun was less affected by urban expansion. However, Azevedo et al. (2016) used MODIS LST to identify the spatial pattern of daytime and nighttime UHI in Birmingham, UK, and found that the spatial the SUHI at nighttime is very similar to daytime. The regional geographic, environment and weather conditions are important in meso-scale UHI studies, which may help to explain the various temperature patterns.

Urbanization reflects growth in size, height, and density (Yang et al., 2017). The UHI effect is often linked to the constant increase in city density, and is often most pronounced in city's most densest parts (Debbage and Shepherd, 2015; Mohajerani et al., 2017). Impervious surface is the most significant factors contributing to LST, and thereby the UHI effect (Chapman et al., 2017). Many studies have observed statistically positive linear relationships between the LST and impervious surface areas or NDBI (Morabito et al., 2016; Wang et al., 2018; Wu et al., 2019). Investigation with the MODIS LST products can provide insights into the varying associations between built-up areas and LST during both daytime and nighttime. Research on this topic for northeast China is, however, still lacking. In this research, using PLR, the responses of LST to built-up density during both daytime and nighttime, and its thresholds were detected (Fig. 5). Overall, high built-up density (i.e., above 70%–80% at daytime and 40%–50% at nighttime) has greater effects on the LST with the intensifying urbanization, and the nighttime LST is more sensitive to a critical built-up density; that is, when built-up

density reaches its threshold, the LST would increased sharply with increasing built-up density, and such phenomenon is important for mitigation strategies of the nighttime UHI effects. The various factors need to be explored in such difference in response of LST to built-up density between day and night time in further research, which is significant for mitigating the UHI effect in Changchun city. In addition, these results suggest that a tipping point of built-up density may occur, where there is a significant influence on the regional thermal environment; however, such breakpoints may vary in cities.

The spatial heterogeneity of both daytime and nighttime LST generally exists in urban areas (Fig. 6). The analysis of the RFDs of the LST reveals that rapid urban expansion resulted in a decrease in heterogeneity of daytime LST in both the existing and newly urbanized areas, and nighttime LST in existing urban area as well. In addition, urban expansion had a positive effect on mean LST in many newly, continually urbanized area, especially at daytime. Previous research claimed that as cities grew, surface temperatures rose higher in newly urbanized areas than existing areas, and even in some cases remained the same (Coutts et al., 2008; Trusilova et al., 2013). In this study, we found that urban expansion increased the mean nighttime NLST, and the relative frequency of high temperature in the existing urban area during 2000–2020, creating a warmer urban core than the rest of the developed areas during the nighttime. However, urban expansion can hardly explain the LST variation at daytime in the existing urban area. Even temperatures did rise in pre-existing urban areas, the temperature change was smaller (Chapman et al., 2017). Thus, it is still necessary to consider the combined effects of various factors contributing to urban thermal environment, such as anthropogenic heat release and climate change. Anthropogenic heat release, released from human activities such as traffic, can increase the UHI by 3℃ , and by greater in densely populated urban areas (Bohnenstengel et al., 2014). Also, local UHIs are affected by climate change, including (in any direction) changes to clouds, wind speeds, and soil dryness (Chapman et al., 2017). Additionally, increases in UHI may be related to growth in the vertical dimension of urban densification, with building height (Mahtta et al., 2019). Urban densification counteracts the negative effects of intense urbanization, but creates pressure on the inner-city environment caused by increased population density, UHI effects and/or heat wave susceptibility (Lemonsu et al., 2015; Chen et al., 2020).

4.4 Implications and Limitations

Urban expansion is a crucial driving force behind changes in urban thermal environment that cannot be ignored. The findings in this research have important implications for the mitigation of UHI effect with the intensifying urbanization. The varying effects of urban expansion on the thermal environment between day and night time were analyzed, and the crucial thresholds of LST in response to built-up density were detected. The LST variation appear to be sensitive and highly magnified with intensifying urbanization, especially in many continually urbanized areas, and thus, it is critical and valuable for rational urban planning and sustainable development in terms of mitigating the UHI effects.

There exist some limitations in this study. The underlying mechanism of the varying effects of urban land expansion on urban thermal environment between day and night time needs to be further explored for better UHI mitigation. Morever, since urbanization is a multifaceted process linked to population growth, modernization, industrialization, and the sociological process of rationalization, and therfore, how urbanization coupled with other factors affect the thermal environment in cities need further enhancement, for better serving as a useful policy guide for city planners and policy makers.

5 Conclusions

Urban expansion has been shown to be the most significant cause of the UHI effect globally. This study examined the spatial and temporal changes in urban land expansion and the thermal environment in proper of Changchun City, Northeast China from 2000 to 2020, using MODIS 8-d LST data, multitemporal Landsat data, and statistical approaches. The relationships between LST and built-up density during both daytime and nighttime were quantitatively modeled, with the detection of crucial thresholds, and the varying effects of urban expansion on the LST between day and night time were analyzed in this study.

Analysis of urban land expansion showed that Changchun experienced rapid urban expansion from

2000 to 2020, with urban built-up areas increasing from 171.77 to 525.14 km^2. Accompanied with urbanization, areas of heat island increased profoundly during both daytime and nighttime, especially for most intensive heat island. In particular, the spatial distribution of daytime LST was more clearly linked to urban expansion than that of nighttime LST. Using PLR, a positive linear correlation of built-up density to the LST was found, with critical breakpoints of 70%–80% during the daytime and 40%–50% at nighttime, which are important for mitigation of heating effect. Above the critical density, the increasing built-up density has greater effects on the LST with the intensifying urbanization, especially at nighttime.

The analysis of the RFDs of the LST reveals the rapid urbanization significantly affected the spatial heterogeneity of the LST, resulting in a decrease of LST spatial heterogeneity in existing urban area, especially at daytime. However, it had an opposite effect on the spatial heterogeneity of the LST in newly urbanized areas between day and night time, that decreased the spatial heterogeneity of LST during the daytime but increased at nighttime. In addition, urban expansion significantly increased the mean LST in newly urbanized areas, especially at daytime, but had weak effects on temperature in the existing urban area. This research helps to better understand the magnitude and spatial variability of the urban thermal environment caused by urban expansion, and can provide some useful reference for urban designers and developers.

References

Azevedo A, Chapman L, Muller C L, 2016. Quantifying the daytime and night-time urban heat island in Birmingham, UK: a comparison of satellite derived land surface temperature and high resolution air temperature observations. *Remote Sensing*, 8(2): 153. doi: 10.3390/rs8020153

Bohnenstengel S I, Hamilton I, Davies M et al., 2014. Impact of anthropogenic heat emissions on London's temperatures. *Quarterly Journal of the Royal Meteorological Society*, 140(679): 687–698. doi: 10.1002/qj.2144

Chapman S, Watson J E M, Salazar A et al., 2017. The impact of urbanization and climate change on urban temperatures: a systematic review. *Landscape Ecology*, 32(10): 1921–1935. doi: 10.1007/s10980-017-0561-4

Chen L, Ren C Y, Zhang B et al., 2018. Quantifying urban land sprawl and its driving forces in Northeast China from 1990 to 2015. *Sustainability*, 10(1): 188. doi: 10.3390/su10010188

Chen T H K, Qiu C P, Schmitt M et al., 2020. Mapping horizontal and vertical urban densification in Denmark with Landsat time-series from 1985 to 2018: a semantic segmentation solution. *Remote Sensing of Environment*, 251: 112096. doi: 10.1016/j.rse.2020.112096

Coutts A M, Beringer J, Tapper N J, 2008. Investigating the climatic impact of urban planning strategies through the use of regional climate modelling: a case study for Melbourne, Australia. *International Journal of Climatology*, 28(14): 1943–1957. doi: 10.1002/joc.1680

Debbage N, Shepherd J M, 2015. The urban heat island effect and city contiguity. *Computers, Environment and Urban Systems*, 54: 181–194. doi: 10.1016/j.compenvurbsys.2015.08.002

Deilami K, Kamruzzaman, Liu Y, 2018. Urban heat island effect: a systematic review of spatio-temporal factors, data, methods, and mitigation measures. *International Journal of Applied Earth Observation and Geoinformation*, 67: 30–42. doi: 10.1016/j.jag.2017.12.009

Dobrovolný P, 2013. The surface urban heat island in the city of Brno (Czech Republic) derived from land surface temperatures and selected reasons for its spatial variability. *Theoretical and Applied Climatology*, 112(1–2): 89–98. doi: 10.1007/s00704-012-0717-8

Duncan J M A, Boruff B, Saunders A et al., 2019. Turning down the heat: an enhanced understanding of the relationship between urban vegetation and surface temperature at the city scale. *Science of The Total Environment*, 656: 118–128. doi: 10.1016/j.scitotenv.2018.11.223

Estoque R C, Murayama Y, Myint S W, 2017. Effects of landscape composition and pattern on land surface temperature: an urban heat island study in the megacities of Southeast Asia. *Science of the Total Environment*, 577: 349–359. doi: 10.1016/j.scitotenv.2016.10.195

Fernández I C, Wu J G, 2016. Assessing environmental inequalities in the city of Santiago (Chile) with a hierarchical multiscale approach. *Applied Geography*, 74: 160–169. doi: 10.1016/j.apgeog.2016.07.012

Hu X F, Zhou W Q, Qian Y G et al., 2017. Urban expansion and local land-cover change both significantly contribute to urban warming, but their relative importance changes over time. *Landscape Ecology*, 32(4): 763–780. doi: 10.1007/s10980-016-0484-5

Huete A R, 1988. A soil-adjusted vegetation index (SAVI). *Remote Sensing of Environment*, 25(3): 295–309. doi: 10.1016/0034-4257(88)90106-X

Huang Huanchun, Yun Yingxia, Wang Shizhen et al., 2014. An analysis of landscape evolution for the thermal comfort degree affected by urban heat island effect. *Journal of Harbin Institute of Technology*, 46(10): 99–105. (in Chinese)

Kuang W H, 2020. 70 years of urban expansion across China: Trajectory, pattern, and national policies. *Science Bulletin*, 65(23): 1970–7974. doi: 10.1016/j.scib.2020.07.005

Kuang W H, Liu J Y, Dong J W et al., 2016. The rapid and massive urban and industrial land expansions in China between

1990 and 2010: a CLUD-based analysis of their trajectories, patterns, and drivers. *Landscape and Urban Planning*, 145: 21–33. doi: 10.1016/j.landurbplan.2015.10.001

Kuang W H, Yan F Q, 2018. Urban structural evolution over a century in Changchun city, Northeast China. *Journal of Geographical Sciences*, 28(12): 1877–1895. doi: 10.1007/s11442-018-1569-7

Lemonsu A, Viguié V, Daniel M et al., 2015. Vulnerability to heat waves: impact of urban expansion scenarios on urban heat island and heat stress in Paris (France). *Urban Climate*, 14: 586–605. doi: 10.1016/j.uclim.2015.10.007

Li C, Zhao J, Xu Y, 2017. Examining spatiotemporally varying effects of urban expansion and the underlying driving factors. *Sustainable Cities and Society*, 28: 307–320. doi: 10.1016/j.scs.2016.10.005

Li G D, Sun S, Fang C L, 2018. The varying driving forces of urban expansion in China: insights from a spatial-temporal analysis. *Landscape and Urban Planning*, 174: 63–77. doi: 10.1016/j.landurbplan.2018.03.004

Li Yuanzheng, Wang Lan, Zhang Liping et al., 2019. Monitoring intra-annual spatiotemporal changes in urban heat islands in 1449 cities in China based on remote sensing. *Chinese Geographical Science*, 29(6): 905–916. doi: 10.1007/s11769-019-1080-9

Liu Y X, Peng J, Wang Y L, 2018. Efficiency of landscape metrics characterizing urban land surface temperature. *Landscape and Urban Planning*, 180: 36–53. doi: 10.1016/j.landurbplan.2018.08.006

Mahtta R, Mahendra A, Seto K C, 2019. Building up or spreading out? Typologies of urban growth across 478 cities of 1 million+. *Environmental Research Letters*, 14(12): 124077. doi: 10.1088/1748-9326/ab59bf

Mathew A, Khandelwal S, Kaul N, 2017. Investigating spatial and seasonal variations of urban heat island effect over Jaipur city and its relationship with vegetation, urbanization and elevation parameters. *Sustainable Cities and Society*, 35: 157–177. doi: 10.1016/j.scs.2017.07.013

Menberg K, Bayer P, Zosseder K et al., 2013. Subsurface urban heat islands in German cities. *Science of the Total Environment*, 442: 123–133. doi: 10.1016/j.scitotenv.2012.10.043

Meng Q Y, Zhang L L, Sun Z H et al., 2018. Characterizing spatial and temporal trends of surface urban heat island effect in an urban main built-up area: a 12-year case study in Beijing, China. *Remote Sensing of Environment*, 204: 826–837. doi: 10.1016/j.rse.2017.09.019

Mohajerani A, Bakaric J, Jeffrey-Bailey T, 2017. The urban heat island effect, its causes, and mitigation, with reference to the thermal properties of asphalt concrete. *Journal of Environmental Management*, 197: 522–538. doi: 10.1016/j.jenvman.2017.03.095

Morabito M, Crisci A, Messeri A et al., 2016. The impact of built-up surfaces on land surface temperatures in Italian urban areas. *Science of the Total Environment*, 551–552: 317–326. doi: 10.1016/j.scitotenv.2016.02.029

Pal S, Ziaul S, 2017. Detection of land use and land cover change and land surface temperature in English Bazar urban centre. *The Egyptian Journal of Remote Sensing and Space Science*, 20(1): 125–145. doi: 10.1016/j.ejrs.2016.11.003

Peng J, Tian L, Liu Y X et al., 2017. Ecosystem services response to urbanization in metropolitan areas: thresholds identification. *Science of the Total Environment*, 607–608: 706–714. doi: 10.1016/j.scitotenv.2017.06.218

Peng J, Xie P, Liu Y X et al., 2016. Urban thermal environment dynamics and associated landscape pattern factors: a case study in the Beijing metropolitan region. *Remote Sensing of Environment*, 173: 145–155. doi: 10.1016/j.rse.2015.11.027

Schwarz N, Lautenbach S, Seppelt R, 2011. Exploring indicators for quantifying surface urban heat islands of European cities with MODIS land surface temperatures. *Remote Sensing of Environment*, 115(12): 3175–3186. doi: 10.1016/j.rse.2011.07.003

Sekertekin A, Abdikan S, Marangoz A M, 2018. The acquisition of impervious surface area from LANDSAT 8 satellite sensor data using urban indices: a comparative analysis. *Environmental Monitoring and Assessment*, 190(7): 381. doi: 10.1007/s10661-018-6767-3

Singh P, Kikon N, Verma P, 2017. Impact of land use change and urbanization on urban heat island in Lucknow city, Central India. *A remote sensing based estimate. Sustainable Cities and Society*, 32: 100–114. doi: 10.1016/j.scs.2017.02.018

Sun Y, Zhao S Q, Qu W Y, 2015. Quantifying spatiotemporal patterns of urban expansion in three capital cities in Northeast China over the past three decades using satellite data sets. *Environmental Earth Sciences*, 73(11): 7221–7235. doi: 10.1007/s12665-014-3901-6

Sun Y W, Gao C, Li J L et al., 2018. Examining urban thermal environment dynamics and relations to biophysical composition and configuration and socio-economic factors: a case study of the Shanghai metropolitan region. *Sustainable Cities and Society*, 40: 284–295. doi: 10.1016/j.scs.2017.12.004

Tan M H, Li X B, 2015. Quantifying the effects of settlement size on urban heat islands in fairly uniform geographic areas. *Habitat International*, 49: 100–106. doi: 10.1016/j.habitatint.2015.05.013

Tsai Y H, 2005. Quantifying urban form: compactness versus 'sprawl'. *Urban Studies*, 42(1): 141–161. doi: 10.1080/00420980420003097 48

Trusilova K, Früh B, Brienen S et al., 2013. Implementation of an urban parameterization scheme into the regional climate model COSMO-CLM. *Journal of Applied Meteorology and Climatology*, 52(10): 2296–2311. doi: 10.1175/JAMC-D-12-0209.1

Wang Y C, Hu B K H, Myint S W et al., 2018. Patterns of land change and their potential impacts on land surface temperature change in Yangon, Myanmar. *Science of the Total Environment*, 643: 738–750. doi: 10.1016/j.scitotenv.2018.06.209

Wu X L, Li B X, Li M et al., 2019. Examining the relationship between spatial configurations of urban impervious surfaces and land surface temperature. *Chinese Geographical Science*,

29(4): 568–578. doi: 10.1007/s11769-019-1055-x

Xu H Q, 2008. A new index for delineating built-up land features in satellite imagery. *International Journal of Remote Sensing*, 29(14): 4269–4276. doi: 10.1080/01431160802039957

Yang C B, He X Y, Yan F Q et al., 2017. Mapping the influence of land use/land cover changes on the urban heat island effect—a case study of Changchun, China. *Sustainability*, 9(2): 312. doi: 10.3390/su9020312

Yang C B, Yan F Q, Lei X L et al., 2020. Investigating seasonal effects of dominant driving factors on urban land surface temperature in a snow-climate city in China. *Remote Sensing*, 12(18): 3006. doi: 10.3390/rs12183006

Yeh C T, Huang S L, 2009. Investigating spatiotemporal patterns of landscape diversity in response to urbanization. *Landscape and Urban Planning*, 93(3–4): 151–162. doi: 10.1016/j.landurbplan.2009.07.002

Yue W Z, Liu X, Zhou Y Y et al., 2019. Impacts of urban configuration on urban heat island: An empirical study in China megacities. *Science of The Total Environment*, 671: 1036–1046. doi: 10.1016/j.scitotenv.2019.03.421

Zhang X Y, Zhong T Y, Feng X Z et al., 2009. Estimation of the relationship between vegetation patches and urban land surface temperature with remote sensing. *International Journal of Remote Sensing*, 30(8): 2105–2118. doi: 10.1080/01431160802549252

Zhou D C, Zhao S Q, Zhang L X et al., 2015. The footprint of urban heat island effect in China. *Scientific Reports*, 5: 11160. doi: 10.1038/srep11160

Zhou D C, Zhang L X, Hao L et al., 2016. Spatiotemporal trends of urban heat island effect along the urban development intensity gradient in China. *Science of the Total Environment*, 544: 617–626. doi: 10.1016/j.scitotenv.2015.11.168